Homology Modeling of a Human Glycine Alpha 1 Receptor Reveals a Plausible Anesthetic Binding Site

Edward J. Bertaccini,*,†,§ Jessica Shapiro,‡ Douglas L. Brutlag,‡ and James R. Trudell†

Department of Anesthesia, Stanford University School of Medicine, Stanford, California 94305-5117, Biophysics Program and Department of Biochemistry, Stanford University, Stanford, California 94305-5307, and Department of Veterans Affairs, Palo Alto VA Health Care System, Palo Alto, California 94304

Received August 23, 2004

The superfamily of ligand-gated ion channels (LGICs) has been implicated in anesthetic and alcohol responses. Mutations within glycine and GABA receptors have demonstrated that possible sites of anesthetic action exist within the transmembrane subunits of these receptors. The exact molecular arrangement of this transmembrane region remains at intermediate resolution with current experimental techniques. Homology modeling methods were therefore combined with experimental data to produce a more exact model of this region. A consensus from multiple bioinformatics techniques predicted the topology within the transmembrane domain of a glycine alpha one receptor (GlyRa1) to be alpha helical. This fold information was combined with sequence information using the SeqFold algorithm to search for modeling templates. Independently, the FoldMiner algorithm was used to search for templates that had structural folds similar to published coordinates of the homologous nAChR (1OED). Both SeqFold and Foldminer identified the same modeling template. The GlyRa1 sequence was aligned with this template using multiple scoring criteria. Refinement of the alignment closed gaps to produce agreement with labeling studies carried out on the homologous receptors of the superfamily. Structural assignment and refinement was achieved using Modeler. The final structure demonstrated a cavity within the core of a four-helix bundle. Residues known to be involved in modulating anesthetic potency converge on and line this cavity. This suggests that the binding sites for volatile anesthetics in the LGICs are the cavities formed within the core of transmembrane four-helix bundles.

For many years since the era of Meyer and Overton,[1,2] the mechanisms of anesthetic action were thought to be mediated via the lipid bilayer of cells involved in neuronal pathways fundamental to consciousness. Since that time, there has been much support for the theory that anesthetics mediate their effects by directly interacting with the proteins involved in the transmission of neuronal signals within the central nervous system. The transmembrane ligand-gated ion channels (LGICs) are a class of proteins that are fundamental to the transfer of information within the nervous system and are also very sensitive to the effects of volatile anesthetics.[3] In particular, recent data strongly suggests that alterations in the transmembrane domain (TM) of GABA and glycine receptors are involved in the anesthetic effect mediated by these ion channels.[4,5] Our search for sites of anesthetic action has therefore focused on the problem of modeling these molecular regions within the transmembrane domains of the ligand-gated ion channels.

Most receptor proteins of biological interest are studied after their structure is determined via X-ray crystallography. Because transmembrane proteins such as the ligand-gated ion channels tend to denature upon their removal from their membrane environment, they generally do not form the crystals of their native folded state that would be necessary for X-ray crystallography. Other methods for structure determination, such as cryo-electron microscopy, have only been able to render low to intermediate resolution structural images of these proteins.[6] Therefore, molecular modeling has been used to study such systems for the purposes of analyzing and visualizing both protein structure as well as ligand binding.[7−10]

Recently, an intermediate resolution structure of the homologous nAChR was determined by cryo-electron microscopy (PDB id 1OED).[6] While atomic coordinates were presented, their certainty is currently inadequate for the level of understanding we seek. In fact, the authors note that the published coordinates are preliminary, especially those pertaining to the fourth transmembrane domain (TM4). Importantly, Unwin and co-workers make the following disclaimer within the comments section of the PDB coordinates file itself (PDB id 1OED):[6] "No refinement was carried out on the model. The coordinates are preliminary.... The link between TM1 and TM2 was poorly resolved and the trace here is almost certainly wrong in detail.... Users should bear in mind that because of the limited resolution the conformations of the side chains and their atomic coordinates are not individually reliable. Also the ends of the helices are uncertain by at least one residue."

However, for the first time the new images do reveal the existence of four-helix bundles as the basic transmembrane subunits for the LGICs, confirming our previous predictions.[11] While the 1OED coordinates confirm several aspects of the model we report here, its intermediate resolution is

* Corresponding author phone: (650)493-5000 ext. 65180; fax: (650)-852-3423; e-mail: edwardb@stanford.edu. Corresponding author address: Department of Anesthesia, 112A, Palo Alto VA Health Care System, 3801 Miranda Avenue, Palo Alto, CA 94304.

† Department of Anesthesia, Stanford University School of Medicine.

‡ Biophysics Program and Department of Biochemistry, Stanford University.

§ Palo Alto VA Health Care System.

10.1021/ci0497399 CCC: $30.25
Published on Web 12/02/2004

insufficient for homology modeling, and, unlike our model, it cannot explain several salient points that are paramount to the mechanism of anesthesia. Here, we have utilized two completely independent techniques to search for a high-resolution four-helix bundle as a template for purposes of modeling the glycine alpha 1 receptor (GlyRa1). The SeqFold technique combines sequence and fold information to search for a modeling template. The Foldminer algorithm actually uses the coordinates of 1OED to find a similar 3D structure with higher resolution coordinates to be used as a basis for modeling. In our work, the two independent techniques agree on the same high-resolution template. Subsequent homology modeling has resulted in a model that shows well-packed alpha helices that surround a central cavity. Amino acid residues known to be involved in the anesthetic effect on these ion channels line this cavity, thereby forming an anesthetic binding pocket. While our previous work has alluded to the presence and location of such a cavity, the current work demonstrates the anesthetic binding cavity from a more robust consensus of multiple algorithms. This allows for a more detailed description of such a cavity's characteristics than in any of our previous works.

METHODS

BLAST and FASTA Search for Modeling Template. The amino acid sequence of the human GlyRa1 was obtained from the National Center for Biotechnology Institute (NCBI). Its NCBI PID accession number is g121576 and its Swiss-Prot accession number is P23415. The sequence was edited to remove the initial 28 amino acid signal peptide component. All subsequent amino acid numbering is based on the mature sequence without the signal peptide. The sequence of the GlyRa1 was then edited to remove most of the residues in the TM3-TM4 loop. The long intracellular loop connecting TM3 and TM4 was replaced by six residues, 3 from each TM. This loop segment was chosen because connecting loops with more than five glycine residues do not alter the transition state of folding/refolding in the nearly perfect four-helical bundle of E. coli Repressor Of Primer protein (PDBid 1ROP),[12] and previous molecular dynamics simulations have determined that seven glycine residues were optimum for a helix-loop-helix motif.[13] Initial searches of the database of proteins with known 3D coordinates available at the Research Collaboratory for Structural Biology (PDB) were performed using the FASTA algorithm.[14] Searches for templates were also performed on the sequence database at the National Center for Biotechnology and Information using the BLAST and PSIBLAST algorithms with a variety of input parameters.[15] Despite using an expectation value cutoff as high as 1, these searches did not yield any significant homologue to our edited GlyRa1 sequence based upon sequence characteristics alone, other than the aforementioned 1OED.

Initial SeqFold Search for Modeling Template. We then resorted to performing a search based on both sequence and secondary structure. We have previously predicted that the transmembrane domain subunits of the GlyRa1 (and all members of the "Cys-loop" superfamily of LGICs) are four-helix bundles.[11] The sequence of the GlyRa1 was then annotated with this secondary structure information and used as input for a new search program based on both sequence and fold topology. This program, called SeqFold (Accelrys Inc., San Diego, CA),[16] was used with varying parameters for secondary structure weighting, similarity matrices, and gap penalties to search a sequence database of proteins whose structures have been solved. This database represents a 95% nonredundant subset of the PDB. This database had also been annotated with secondary structure information based on geometric criteria for each sequence position. The results of our searches were rated according to initial SeqFold similarity score, the number of similar amino acids within the helical regions, the number and size of gaps in helical segments, and the proximity of residues in TM1, 2, and 3 that are relevant to anesthetic effect. This process consistently indicated a match to chain A of 2CCY, a heme-containing four-helix bundle ($p = 0.0027$ using a structure to sequence weighting of 3:1).[17] All of the GlyRa1 predicted helical residues align to known helical residues in the 2CCY template. The sequence similarity among helical residues is 42%, while the sequence identity in the same region is 9.5%. Only one gap in the conserved helical regions required closing during the threading process. The initial automatic alignment revealed three residues known to be involved in anesthetic binding at the same relative height along the core axis of the four-helix bundle.

Refined SeqFold Search for Modeling Template. Using the CATH database (http://www.biochem.ucl.ac.uk/bsm/cath/)[18] of proteins categorized based on fold type, 2CCY was then used as input to the VAST search engine[19] at the same Web site in order to perform an expanded and updated search for proteins with a comparable fold. This would then focus the search to four-helix bundles of the up−down fold variety and perhaps find structures not available in the previous database. This search returned 20 hits based on 3D structural similarity. Each of their sequences was then annotated for secondary structure based on geometric criteria from the DSSP[13] algorithm and placed into a database searchable by the SeqFold algorithm.[16] This abridged database of 20 alpha helical bundles was searched using the edited GlyRa1 sequence as input. Subdomain 2 of chain C within the bovine cytochrome *c* oxidase structure (PDB id 2OCC)[20] met the aforementioned criteria within this focused database of four-helix bundles ($p = 0.007$ using a secondary structure sequence weighting of 5:1). Ninety-five percent of the GlyRa1 predicted helical residues align to known helical residues in 2OCC. The sequence identity among helical residues is 10%, while the sequence similarity in the same region is 51%. The alignment contains only two gaps in the conserved helical regions that required closing during the threading process. Two other proteins (2CCY and 256B) were identified as similarly strong matches, but the shorter lengths of the alpha helices made them less suitable as templates for transmembrane domains. The initial automatic alignment produced proximity of the three relevant residues known to be involved in anesthetic binding at the same level within the core of the four-helix bundle. Furthermore, manual searches of both the CATH and SCOP databases of 3D proteins (that are categorized based upon protein fold) show that this portion of 2OCC is the only *mammalian* transmembrane four-helix bundle for which there are well-defined 3D coordinates. We edited the PDB file for 2OCC so that it contained only the four-helical bundle being considered, and hereafter we refer to subdomain two of chain C in cytochrome *c* oxidase as 2OCC-4H.

Foldminer Search for Modeling Template. While the cryo-electron micrograph of the homologous nAChRa1 (PDB id 1OED) may only be of intermediate resolution, it still appears to reveal correct protein fold information and validates our previous transmembrane topology predictions. Therefore, as a completely independent verification of our template selection, we used the FoldMiner algorithm (Brutlag Lab, Stanford University)[21,22] to search for known proteins with folds that are comparable to that published for the intermediate resolution structure of the torpedo nAChRa1. FoldMiner uses LOCK 2, a structural alignment program, to align the query structure to each target in the database and assesses structural similarity at the level of secondary structure elements. It assesses potential alignments by comparing the orientations of aligned secondary structure elements in the query and target structures. This system prefers structural alignments that are global with respect to both the query and target and is devoid of bias or information regarding amino acid sequence. The results of this structural fold-based search gave high scores to several of the same folds generated in the aforementioned SeqFold search, including 2OCC-4H and 256B. Again, 2OCC-4H was chosen due to the greater number of structurally aligned helical residues, and a homology model was subsequently constructed.

Homology Modeling. The edited sequence of the GlyRa1 was initially aligned with the 2OCC-4H template, as suggested in the initial SeqFold output. It was further refined based on the mean force potential of Sippl[23] present within the SwissPDB Viewer software package (GlaxoSmithKline R&D and the Swiss Institute of Bioinformatics).[24] Final refinement of alignments and gap closure were based upon experimental criteria from site-directed mutations and labeling studies. The Modeler module within the Insight II software suite (Accelrys Inc., San Diego, CA) was then utilized to assign atomic coordinates to regions structurally aligned with the template, build intervening loops, optimize the rotamers of amino acid side chains, and perform an initial energy optimization of the structure. CASTp (http://cast.engr.uic.edu/cast/)[25] and the Binding Site Analysis module of Insight II (Accelrys Inc., San Diego, CA) were then used to identify all cavities associated with the model as well as measure the volume they contain. These programs were used to search for cavities that lie within the subunits and are bounded by residues Ile229, Ser267, and Ala288. Phi-psi angle analysis was carried out using the Ramachandran plot capabilities of the VMD software package (Theoretical and Computational Biophysics Group and the NIH Resource for Macromolecular Modeling and Bioinformatics).[26] An initial search for amino acid clashes was performed with the SwissPDB Viewer software package (GlaxoSmithKline R&D and the Swiss Institute of Bioinformatics).[24] Residue polarity and lipophilicity profiles as well as electrostatic potential mapping to the Connelly solvent accessible surface was carried out using DS Modeling Viewer v. 5.0 (Accelrys, San Diego, Ca.).

RESULTS

Helical Dimensions and Packing. The alpha helices within our model average 23 amino acid residues in length. This is long enough to span the typical lipid bilayer thickness, even if the helices are oriented at a slight angle to the bilayer normal. The limits of these helices in the GlyRa1 are approximately as follows: TM1: 225−245; TM2: 249−272; TM3: 280−303; TM4: 396−418 (Figure 1A).

A Ramachandran plot clearly shows the vast majority of the membrane-spanning amino acids are in a phi-psi distribution consistent with right-handed alpha helices. The remaining residues that fall into the random or beta configuration geometries are very short segments and are primarily in the loop regions of the protein (Figure 2A). A quick check of amino acid side chain integrity did not reveal any amino acid side chain clashes with one another or with the backbone.

The helices are reasonably well packed without gross spaces between them when studied as a space-filling model (Figure 1B). The crossing of the helices in a left-handed four-helical bundle produces a funnel shaped cavity within the core of the four-helix bundle. This cavity has access to the outside of the bundle through gaps in the helical packing on both sides of TM4 (Figure 1C,D). The cavity volume estimated by CASTp[25] was dependent on the radius of the probe sphere; a probe radius of 1.4 Å outlined a cavity of 545 Å^3, while a probe radius of 1.65 Å outlined a cavity of 470 Å^3. The cavity volume measured by Binding Site Analysis was dependent on the maximum distance between grid points exposed at the aperture to the cavity; the default value of 7 Å outlined a cavity of 340 Å^3, whereas a value of 5 Å decreased the volume to 221 Å^3.

Other potential templates for model building were identified as noted above. Despite their overall search scores and residue alignments differing somewhat from those for the template finally chosen, models were built nonetheless from these other templates for the sake of comparison. These other templates include the proteins known in PDB notation as 2CCY chain a and 256B. While models made from these templates did satisfy some of the experimental data regarding labeling of various residues, the template structures include a heme moiety between the TM1 and TM4 helices. When the heme is removed, it creates a large cleft between TM1 and TM4 and results in unusual helical packing for our model. We also examined the 1ROP structure mentioned above as a template, in light of its near perfect four helical bundle geometry.[12] This also did not produce satisfactory alignment of residues with experimentally known characteristics and the helices were too short for a membrane-spanning domain.

Proximity of Amino Acids Involved in the Anesthetic Effect. Several amino acids known to modulate anesthetic potency, Ile229, Ser267, and Ala288 line the cavity (Figure 1D) formed within the four-helix bundle. These residues are located at approximately the same level along the bilayer normal and appear to form a portion of a funnel shaped cavity within the outer third of the membrane spanning subunit. Residues from TM4 that are at the same level include the segment from Tyr406 to Tyr410. Several amino acid positions that have been implicated in ion selectivity, Met246-Ala 251 in GlyRa1 (homologous to Ala234-Glu238 in the nAchRa7),[27,28] are in the correct position within the TM1−2 loop that forms the selectivity filter.

Location of Residues Known to Exist in Certain Environments. Residues with well-defined environments, based upon a consensus of experimental site-directed mutations and labeling studies from homologous proteins in the

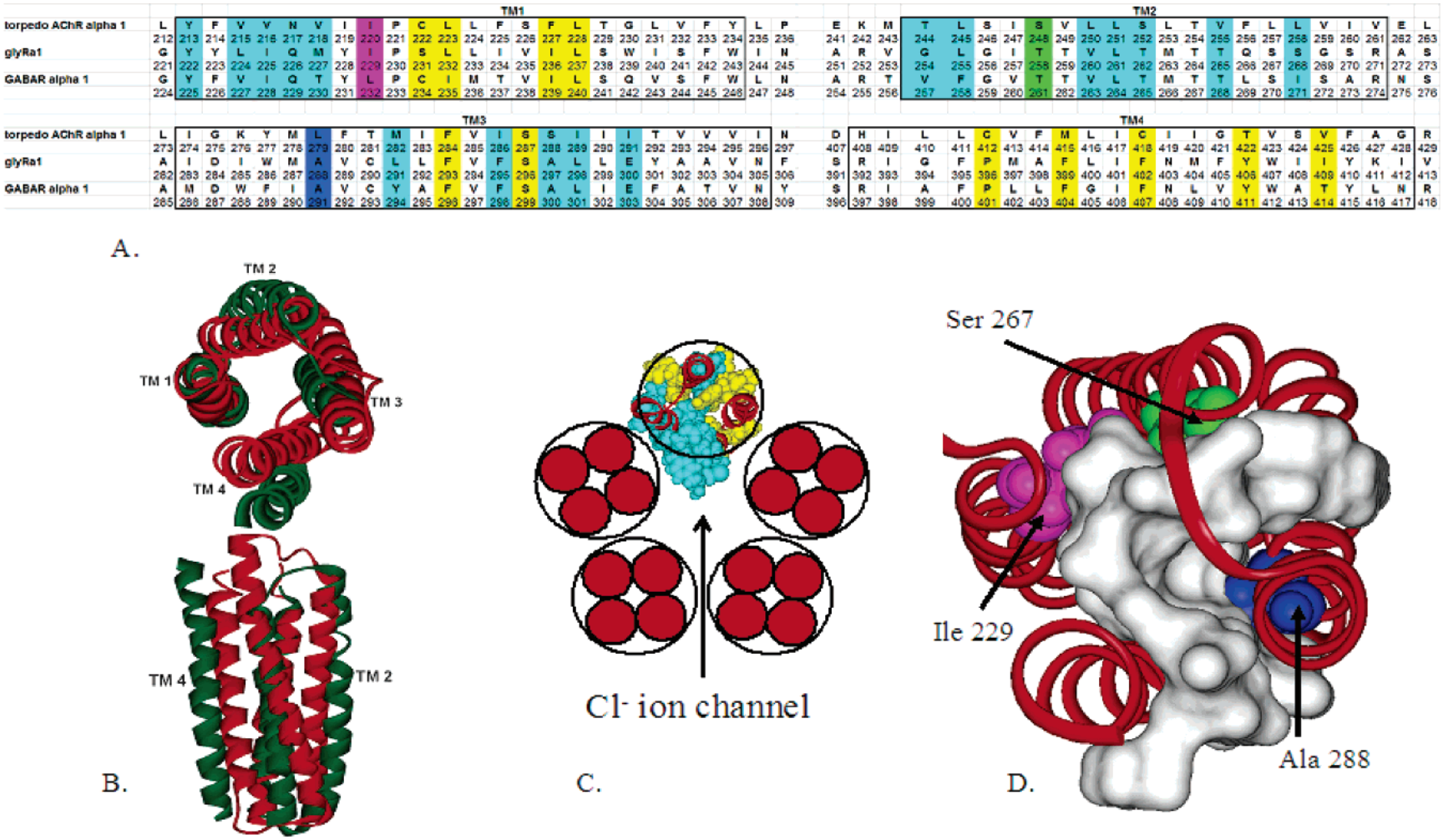

Figure 1. (A) Multiple sequence alignment of torpedo nAChR with human glyRa1 and GABARa1. The homologous positions of residues exposed to hydrophilic labels (light blue) and hydrophobic labels (yellow) as well as residues involved in anesthetic binding Ile 229 (pink), Ser 267 (green), and Ala 288 (blue) are highlighted. (B) The overlap of 2OCC chain c (red ribbon) with 1OED (green ribbon). Note the better packing of TM4 in 2OCC. (C) Tetramer showing the location of hydrophilic (light blue) and hydrophobic (yellow) positions when arranged into a pentamer of tetramers. Note the general orientation of hydrophilic positions toward the ion poor and hydrophobic residues toward the lipid bilayer. (D) Anesthetic binding caviity (void volume in gray) within the transmembrane alpha helical subunit lined by anesthetic binding residues Ile 229 (pink), Ser 267 (green), and Ala 288 (blue).

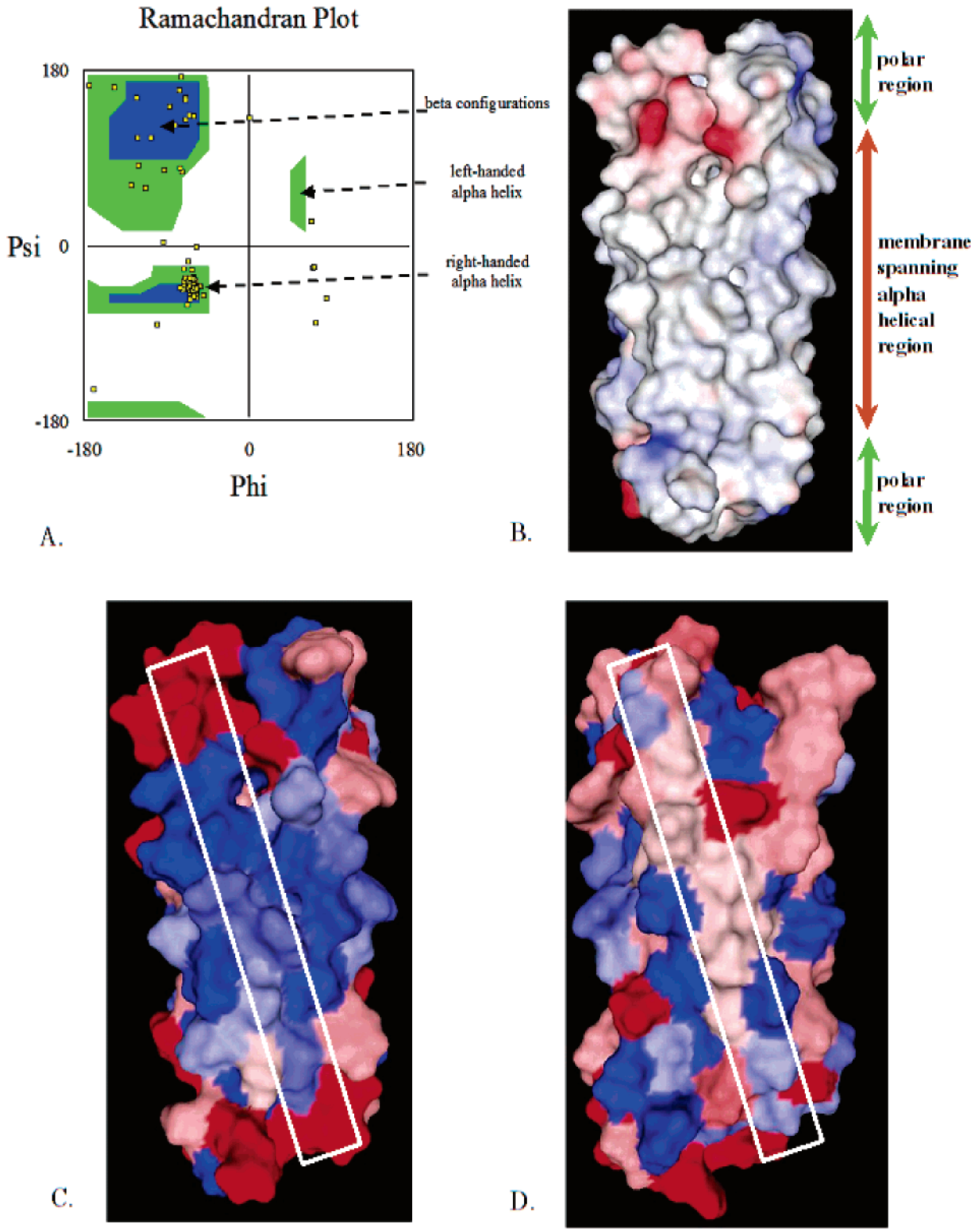

Figure 2. (A) Ramchandran plot showing the majority of amino acids in the phi-psi domain of the right-handed alpha helix. (B) Electrostatic potential surface representation of the glyRa1 (red = negative potential, blue = positive potential). (C) Lipophilic residues looking toward TM4 (outlined in white, blue = more lipophilic, red = less lipophilic). (D) Lipophilic residues looking toward TM2 (outlined in white, blue = more lipophilic, red = less lipophilic) from within the ion channel pore.

superfamily of LGICs, are in reasonable positions. They would tend to face their respective hydrophilic and hydrophobic environments once the four-helix bundle subunits are reconstituted into their pentameric arrangement around a central ion channel. Amino acid positions labeled by mostly hydrophilic reagents are accessible to an aqueous environment.[29−31] Amino acids labeled by mostly hydrophobic reagents would be accessible to the environment of the lipid bilayer or adjacent interhelical appositions (Figure 1A,C).[32,33]

A surface representation of our protein subunit that is color coded by polarity and hydrophobicities also shows several reassuring features. The solvent accessible surface that is color-coded by electrostatic potential (Figure 2B) clearly shows the majority of positive and negative potential on the

surface of the extracellular and cytoplasmic ends of the protein. The same surface color coded by lipophilicity (Figure 2C) demonstrates that the majority of membrane spanning amino acids in TMs 1, 3, and 4 are hydrophobic in nature. However, it should be noted that the membrane spanning amino acids in TM 2 are notably polar when examined from the side facing what would constitute the protein ion channel (Figure 2D). This is appropriate and consistent with these residues lining the water-filled central ion pore of this protein channel as seen in Figure 1C.

DISCUSSION

Our model of the GlyRa1 subunit was constructed using comparative modeling based on a four-helical bundle template. This model accounts for a large body of experimental data, including the alpha helical nature of the transmembrane domain, the appropriate orientation of residues from specific types of labeling experiments, and the location of residues implicated in ion selectivity. Additionally, this model identifies a binding site for anesthetics and alcohols by demonstrating a common cavity that is bounded by residues known to alter the anesthetic sensitivity of the channel. While our current model agrees with the overall topology of the recently published coordinates of the homologous nAChR (PDB id 1OED), it uniquely explains several phenomena not otherwise accounted for by these coordinates (see below).

The Alpha Helical Nature of the Transmembrane Region. The lengths and locations of the helices are very close to those predicted by both our previous transmembrane topology consensus predictions[11] as well as those of the recently published, intermediate resolution coordinates of the homologous nAChR.[6] This has been a very controversial point over the last several years due to a variety of contradictory experimental studies regarding the exact topology and secondary structure of this membrane-spanning region within the LGICs. A substituted cysteine accessibility method (SCAM) study implied that at least part of TM1 is a beta strand.[34] This study involved sequential site-directed mutations of amino acid residues to cysteine followed by reaction with a methanethiosulfonate reagent. Interpretations of recent proteolytic digestion studies also suggest that TM1 and TM3 are of significant beta sheet character.[35,36] Ortells and Lunt previously could not model the transmembrane domain as a purely alpha helical structure due to unfavorable steric interactions of adjacent subunits.[37] As a result, they suggested that an alpha helical structure was unlikely for that domain. Le Novere et al. used secondary structure prediction tools that were trained on globular, water-soluble proteins to infer that the transmembrane region of the LGICs has significant beta sheet structure.[38] Initially, Unwin and co-workers could only discern TM2 as an alpha helix on their cryo-electron micrographs.[39] As a result, they suggested that the other segments *could* be beta strands.

However, we utilized 10 state of the art topology prediction algorithms that are specific for transmembrane environments to show that the subunits of this class of receptors were four-helix bundles of the up−down fold class.[11] This prediction has been supported by isolation, proteolytic digestion, and FTIR analysis of the homologous region within the nAChR.[40] We have also successfully created full models of the transmembrane ion pore (a pentamer of four-helix bundles composed of 20 alpha helices in total) by packing the subunits described here into a pentameric arrangement without encountering the grossly unfavorable steric overlaps noted by others.[3,7,8,41] Finally, though at intermediate resolution, Unwin and co-workers refined their cryo-electron micrograph technique to produce an electron density that could be clearly fit to segments of alpha helices, producing an all-alpha helical topology within the transmembrane domain of the homologous nAChR.[6] Their most recent refinements were made possible after calibrating their technique against the recently published coordinates of the snail acetylcholine binding protein (AChBP),[42] which is homologous to the extramembranous ligand-binding domain of the nAChR.

The Anesthetic Binding Cavity Dimensions. Correlations of anesthetic potencies with anesthetic binding effects are consistently reproduced when anesthetics experimentally interact with well-packed synthetic four-helix bundles[43] such as are present in our model. Site-directed mutations, which systematically varied the volumes of amino acid side chains, indicate that the size of the cavity necessary to accommodate inhalational anesthetics is approximately 250−340 A^3.[4] The volume of the site of action for cyclo alcohols was estimated to be 415 A^3 in tadpoles.[44] The cavity volume estimated in our model (221 A^3 to 554 A^3) is within the range of these experimental results (Figure 1D), though we expect estimates of cavity size to vary since the ion channel is a dynamic structure. In contrast, the current 1OED model has loosely packed alpha helices. It contains a completely different cavity that appears contiguous among all five transmembrane domain subunits, and the cavity is much larger than has been predicted by experiment.

The Anesthetic Binding Cavity Residues and Its Chemical Characteristics. Residues within the transmembrane domains of LGICs have been consistently implicated in the effects of anesthetics and are shown to converge on a common binding cavity within our model (Figure 1D). Ile229 in GlyRa1 and the corresponding Leu232 in GABAaR are important for mediating anesthetic effects.[4] Ser267 in the GlyRa1 and Ser270 in the GABAaR alpha 1 are both at homologous sequence positions on TM2 within a multiple sequence alignment of these receptors. Both of these are involved in the way anesthetics affect these channels.[5] Within TM3, Leu283 in the nAChR alpha 4,[45] Ala288 in the GlyRa1,[5,46] Ala291 in the GABAAR alpha1, and Met286 in the GABAaR beta subunit[47] are all homologous sequence positions within their respective receptors. All of these residues modulate the way in which anesthetics affect ion channels. These homologous amino acid positions have been shown to line a part of the cavity within the core of the alpha helical bundle, converging on an anesthetic binding site.[4,41] Our model implicates residues on TM4 in the range from Tyr 406−410 in the GlyRa1. However, the current experimental data on TM4 is somewhat conflicting and inconclusive regarding a single specific residue pertinent to anesthetic binding.[32,48,49] The most recent data using cysteine scanning mutagenesis and propyl-MTS reagent labeling suggest that residues Trp 407 and Tyr 410 in TM4 are of paramount importance in the anesthetic effect (personal communication from Drs. Ingrid Lobo and Adron Harris). This is readily accounted for by our current model. Additionally, our model has been successfully used to predict residues that are within a reasonable distance for cross-linking studies involving cysteine mutagenesis and disulfide bridge formation in the

GlyRa1. Specifically, Ser267 and Ala288 have been clearly shown to be near neighbors by this technique.[50]

The residues that line the putative anesthetic binding site would also impart a somewhat amphipathic character to the cavity, with serine and tyrosine having the capacity for polar/hydrogen bond interactions, whereas alanine and isoleucine are capable of more hydrophobic interactions. The latter group of residues may satisfy the Meyer-Overton correlation of anesthetic potency and lipid solubility.[1,2] The possibility for hydrophilic interactions satisfies the potency correlations of the fluoroalkanes and fluoroalkanols studied by Eger and co-workers.[51−53] The recently published intermediate resolution coordinates of the nAChR (1OED) display the appropriate orientation of the residue homolgous to Ser267 on TM2.[6] However, the remaining residues in the nAChR model that are homologous to those known to be involved in anesthetic action are not in proximity to one another[50] and do not form a common site into which anesthetics may bind.

While our model explains the location of several key amino acids that have been consistently identified as being involved in the volatile anesthetic effect, there are other amino acid effects that at this point our current model may only partially serve to explain. Dr. Keith Miller's lab has used azietomidate and azioctanol for photolabeling experiments to identify amino acid residues possibly involved in mediating the anesthetic effect of etomidate and octanol. The residue identified as important for octanol binding in the nAChR is alpha Glu262.[54] Those residues relevant to etomidate binding include nAChR alpha Glu262 and nAChR delta Gln276 (both homologous to Ala272 in GlyRa1) within the extracellular end of the nAChR ion channel in the desensitized state, and nAChR delta Ser258 (homologous to Gly254 in GlyRa1) and nAChR delta Ser262 (homologous to Thr 258 in GlyRa1), toward the cytoplasmic end.[55] The latter residues are quite distant from the proposed anesthetic binding site and may be, in fact, additional binding sites for etomidate. The residues closer to the extracellular end of the subunit appear just beyond the end of the proposed alpha helices and are located in the beginning of the TM2−3 loop. Binding at this site would not only give a ligand access to the loop, which is implicated in conducting ligand binding information to the transmembrane domain for channel opening, but also access to the upper portion of our proposed anesthetic binding site.

Additionally, halothane photolabeling experiments have identified nAChR delta Tyr228 in the nAChR as relevant to anesthetic binding.[56] This position is homologous to Tyr223 in the GlyRa1, which is also outside of the proposed transmembrane alpha helices and anesthetic binding pocket. However, it is also located in a region that, in our previous models,[7] we have shown is not only important for coupling of the extracellular ligand binding domain to the transmembrane domain but also may have access to the upper most portion of our proposed anesthetic binding pocket.

Access to the Anesthetic Binding Cavity. Last, our model demonstrates that anesthetics may gain access to this binding cavity within the core of the four-helix bundle subunit by either diffusing in from an interfacial site located at the junction of hydrophobic and hydrophilic environments in the membrane or directly through the lipid bilayer (Figure 1D). The latter site may also partially account for the Meyer-Overton correlation of anesthetic potency and lipid solubility.[1,2]

The construct of our proposed anesthetic binding site is quite distinct from that initially put forth by Unwin and colleagues[6] and then expanded upon by Barrantes.[57] Their speculation is that within the homologous nAChR there exists an "outer shell" composed of TMs 1, 3, and 4 from each subunit and an "inner core" composed of TM2 from each subunit. This should be reinterpreted in light of our current model. In particular, we show better packing of TM4 and an anesthetic binding site that is distinct within each individual subunit, not somehow part of a large contiguous space between an inner and outer protein shell. This has important implications for how we think anesthetics may access an anesthetic binding site as well as how the channel opens and closes.

CONCLUSION

In summary, using modern techniques of bioinformatics, computational chemistry, and molecular modeling, we have built a model of the transmembrane subunit region within a human GlyRa1 that accounts for a large body of physicochemical and experimental data that characterizes this region. Most notably, the cavity within this region demonstrates the proximity of amino acid residues known to be involved in the effects of anesthetics on these ion channels, thereby forming a plausible anesthetic binding site. While our previous work has alluded to the presence of such a cavity, this work demonstrates its presence from a more robust derivation using a consensus of multiple algorithms. Furthermore, this model demonstrates a distinct anesthetic binding site with multiple experimentally verified characteristics that are not fully accounted for by the recently published intermediate resolution structure of the nAChR.

ACKNOWLEDGMENT

This work was supported by the Department of Veterans' Affairs, the Stanford University School of Medicine, and the National Institutes of Health grants GM064371 and AA013378.

REFERENCES AND NOTES

(1) Meyer, H. H. Zur Theorie Der Alkoholnarkose. I. Mit Welch Eigenshaft Der Anasthetika Bedingt Ihre Narkotische Wirkung? *Arch. Exp. Path. Pharmakol. (Naunyn Schmiedebergs)* **1899**, *42*, 109−137.

(2) Overton, E. Studien Uber Die Narkose Zugleich Ein Beitrag Zur Allgemeinen Pharmacologie. *Jena, Verlag von Gustav Fischer* 1901.

(3) Yamakura, T.; Bertaccini, E.; Trudell, J. R.; Harris, R. A. Anesthetics and Ion Channels: Molecular Models and Sites of Anesthetic Action. *Annu. Rev. Pharmacol. Toxicol.* **2001**, *41*, 23−51.

(4) Jenkins, A.; Greenblatt, E. P.; Faulkner, H. J.; Bertaccini, E.; Light, A.; Lin, A.; Andreasen, A.; Viner, A.; Trudell, J. R.; Harrison, N. L. Evidence for a Common Binding Cavity for Three General Anesthetics Within the GABAA Receptor. *J. Neurosci.* **2001**, *21*, RC136.

(5) Mihic, S. J.; Ye, Q.; Wick, M. J.; Koltchine, V. V.; Krasowski, M. D.; Finn, S. E.; Mascia, M. P.; Valenzuela, C. F.; Hanson, K. K.; Greenblatt, E. P.; Harris, R. A.; Harrison, N. L. Sites of Alcohol and Volatile Anaesthetic Action on GABA(A) and Glycine Receptors. *Nature* **1997**, *389*, 385−389.

(6) Miyazawa, A.; Fujiyoshi, Y.; Unwin, N. Structure and Gating Mechanism of the Acetylcholine Receptor Pore. *Nature* **2003**, *424*, 949−955.

(7) Trudell, J. R.; Bertaccini, E. Comparative Modeling of a GABAA A1 Receptor Using Three Crystal Structures As Templates. *J. Mol. Graphics Modell.* **2004**, *23*, 39−49.

(8) Trudell, J. R.; Bertaccini, E. Molecular Modelling of Specific and Non-Specific Anaesthetic Interactions. *Br. J. Anaesth.* **2002**, *89*, 32−40.

(9) Sansom, M. S. P. Ion Channels: Molecular Modeling and Simulation Studies. *Methods Enzymol.* **1998**, *293*, 647−693.

(10) Absalom, N. L.; Lewis, T. M.; Schofield, P. R. Mechanisms of Channel Gating of the Ligand-Gated Ion Channel Superfamily Inferred From Protein Structure. *Exp. Physiol.* **2004**, *89*, 145−153.
(11) Bertaccini, E.; Trudell, J. R. Predicting the Transmembrane Secondary Structure of Ligand-Gated Ion Channels. *Protein Eng.* **2002**, *15*, 443−453.
(12) Nagi, A. D.; Anderson, K. S.; Regan, L. Using Loop Length Variants to Dissect the Folding Pathway of a Four-Helix-Bundle Protein. *J. Mol. Biol.* **1999**, *286*, 257−265.
(13) Liu, H. L.; Shu, Y. C.; Wu, Y. H. Molecular Dynamics Simulations to Determine the Optimal Loop Length in the Helix-Loop-Helix Motif. *J. Biomol. Struct. Dyn.* **2003**, *20*, 741−745.
(14) Pearson, W. R.; Lipman, D. J. Improved Tools for Biological Sequence Comparison. *Proc. Natl. Acad. Sci. U.S.A.* **1998**, *85*, 2444−2448.
(15) Altschul, S. F.; Madden, T. L.; Schaffer, A. A.; Zhang, J.; Zhang, Z.; Miller, W.; Lipman, D. J. Gapped BLAST and PSI−BLAST: a New Generation of Protein Database Search Programs. *Nucleic Acids Res.* **1997**, *25*, 3389−3402.
(16) Olszewski, K.; Yan, L.; Edwards, D. J. SeqFold. Fully Automated Fold Recognition and Modeling Software. Evaluation and Application. *Theor. Chem. Acc.* **1999**, *101*, 57−61.
(17) Finzel, B. C.; Weber, P. C.; Hardman, K. D.; Salemme, F. R. Structure of Ferricytochrome C′ From Rhodospirillum Molischianum at 1.67 A Resolution. *J. Mol. Biol.* **1985**, *186*, 627−643.
(18) Orengo, C. A.; Michie, A. D.; Jones, S.; Jones, D. T.; Swindells, M. B.; Thornton, J. M. CATH- -a Hierarchic Classification of Protein Domain Structures. *Structure* **1997**, *5*, 1093−1108.
(19) Gibrat, J. F.; Madej, T.; Bryant, S. H. Surprising Similarities in Structure Comparison. *Curr. Opin. Struct. Biol.* **1996**, *6*, 377−385.
(20) Yoshikawa, S.; Shinzawa-Itoh, K.; Nakashima, R.; Yaono, R.; Yamashita, E.; Inoue, N.; Yao, M.; Fei, M. J.; Libeu, C. P.; Mizushima, T.; Yamaguchi, H.; Tomizaki, T.; Tsukihara, T. Redox-Coupled Crystal Structural Changes in Bovine Heart Cytochrome *c* Oxidase. *Science* **1998**, *280*, 1723−1729.
(21) Shapiro, J.; Brutlag, D. FoldMiner and LOCK 2: Protein Structure Comparison and Motif Discovery on the Web. *Nucleic Acids Res.* **2004**, *32*, W536−W541.
(22) Shapiro, J.; Brutlag, D. FoldMiner: Structural Motif Discovery Using an Improved Superposition Algorithm. *Protein Sci.* **2004**, *13*, 278−294.
(23) Sippl, M. J. Calculation of Conformational Ensembles From Potentials of Mean Force. An Approach to the Knowledge-Based Prediction of Local Structures in Globular Proteins. *J. Mol. Biol.* **1990**, *213*, 859−883.
(24) Guex, N.; Peitsch, M. C. SWISS-MODEL and the Swiss-PdbViewer: an Environment for Comparative Protein Modeling. *Electrophoresis* **1997**, *18*, 2714−2723.
(25) Liang, J.; Edelsbrunner, H.; Woodward, C. Anatomy of Protein Pockets and Cavities: Measurement of Binding Site Geometry and Implications for Ligand Design. *Protein Sci.* **1998**, *7*, 1884−1897.
(26) Humphrey, W.; Dalke, A.; Schulten, K. VMD: Visual Molecular Dynamics. *J. Mol. Graph.* **1996**, *14*, 33−38.
(27) Karlin, A. Emerging Structure of the Nicotinic Acetylcholine Receptors. *Nat. Rev. Neurosci.* **2002**, *3*, 102−114.
(28) Wilson, G. G.; Karlin, A. The Location of the Gate in the Acetylcholine Receptor Channel. *Neuron* **1998**, *20*, 1269−1281.
(29) Arias, H. R.; Trudell, J. R.; Bayer, E. Z.; Hester, B.; McCardy, E. A.; Blanton, M. P. Noncompetitive Antagonist Binding Sites in the Torpedo Nicotinic Acetylcholine Receptor Ion Channel. Structure−Activity Relationship Studies Using Adamantane Derivatives. *Biochemistry* **2003**, *42*, 7358−7370.
(30) Akabas, M. H.; Karlin, A. Identification of Acetylcholine Receptor Channel-Lining Residues in the M1 Segment of the α-Subunit. *Biochemistry* **1995**, *34*, 12496−12500.
(31) Akabas, M. H.; Kaufmann, C.; Archdeacon, P.; Karlin, A. Identification of Acetylcholine Receptor Channel-Lining Residues in the Entire M2 Segment of the α Subunit. *Neuron* **1994**, *13*, 919−927.
(32) Blanton, M. P.; Lala, A. K.; Cohen, J. B. Identification and Characterization of Membrane-Associated Polypeptides in Torpedo Nicotinic Acetylcholine Receptor-Rich Membranes by Hydrophobic Photolabeling. *Biochim. Biophys. Acta* **2001**, *1512*, 215−224.
(33) Blanton, M. P.; Cohen, J. B. Identifying the Lipid−Protein Interface of the Torpedo Nicotinic Acetylcholine Receptor: Secondary Structure Implications. *Biochemistry* **1994**, *33*, 2859−2872.
(34) Karlin, A.; Akabas, M. H. Substituted-Cysteine Accessibility Method. *Methods Enzymol.* **1998**, *293:123−45*, 123−145.
(35) Barrantes, F. J.; Antollini, S. S.; Blanton, M. P.; Prieto, M. Topography of Nicotinic Acetylcholine Receptor Membrane-Embedded Domains. *J. Biol. Chem.* **2000**, *275*, 37333−37339.
(36) Leite, J. F.; Cascio, M. Structure of Ligand-Gated Ion Channels: Critical Assessment of Biochemical Data Supports Novel Topology. *Mol. Cell Neurosci.* **2001**, *17*, 777−792.
(37) Ortells, M. O.; Lunt, G. G. A Mixed Helix-Beta-Sheet Model of the Transmembrane Region of the Nicotinic Acetylcholine Receptor. *Protein Eng.* **1996**, *9*, 51−59.
(38) Le Novere, N.; Corringer, P. J.; Changeux, J. P. Improved Secondary Structure Predictions for a Nicotinic Receptor Subunit: Incorporation of Solvent Accessibility and Experimental Data into a Two-Dimensional Representation. *Biophys. J.* **1999**, *76*, 2329−2345.
(39) Unwin, N. Nicotinic Acetylcholine Receptor at 9 A Resolution. *J. Mol. Biol.* **1993**, *229*, 1101−1124.
(40) Methot, N.; Ritchie, B. D.; Blanton, M. P.; Baenziger, J. E. Structure of the Pore-Forming Transmembrane Domain of a Ligand-Gated Ion Channel. *J. Biol. Chem.* **2001**, *276*, 23726−23732.
(41) Bertaccini, E.; Trudell, J. R. Molecular Modeling of the Transmembrane Regions of Ligand-Gated Ion Channels: Progress and Challenges. *Int. Rev. Neurobiol.* **2001**, *48*, 141−166.
(42) Brejc, K.; van Dijk, W. J.; Klaassen, R. V.; Schuurmans, M.; van Der, O. J.; Smit, A. B.; Sixma, T. K. Crystal Structure of an ACh-Binding Protein Reveals the Ligand-Binding Domain of Nicotinic Receptors. *Nature* **2001**, *411*, 269−276.
(43) Johansson, J. S.; Gibney, B. R.; Rabanal, F.; Reddy, K. S.; Dutton, P. L. A Designed Cavity in the Hydrophobic Core of a Four-α-Helix Bundle Improves Volatile Anesthetic Affinity. *Biochemistry* **1998**, *37*, 1421−1429.
(44) Curry, S.; Moss, G. W.; Dickinson, R.; Lieb, W. R.; Franks, N. P. Probing the Molecular Dimensions of General Anaesthetic Target Sites in Tadpoles (Xenopus Laevis) and Model Systems Using Cycloalcohols. *Br. J. Pharmacol.* **1991**, *102*, 167−173.
(45) Flood, P.; Lin, A. I.; Harrison, N. L. A Point Mutation in the Alpha-4 Subunit Renders a Neuronal Nicotinic ACh Receptor Insensitive to Isoflurane. *Anesthesiology* **1999**, *91*, A755.
(46) Yamakura, T.; Mihic, S. J.; Harris, R. A. Amino Acid Volume and Hydropathy of a Transmembrane Site Determine Glycine and Anesthetic Sensitivity of Glycine Receptors. *J. Biol. Chem.* **1999**, *274*, 23006−23012.
(47) Krasowski, M. D.; Nishikawa, K.; Nikolaeva, N.; Lin, A.; Harrison, N. L. Methionine 286 in Transmembrane Domain 3 of the GABAA Receptor Beta Subunit Controls a Binding Cavity for Propofol and Other Alkylphenol General Anesthetics. *Neuropharmacology* **2001**, *41*, 952−964.
(48) Jenkins, A.; Andreasen, A.; Trudell, J. R.; Harrison, N. L. Tryptophan Scanning Mutagenesis in TM4 of the GABA(A) Receptor Alpha1 Subunit: Implications for Modulation by Inhaled Anesthetics and Ion Channel Structure. *Neuropharmacology* **2002**, *43*, 669−678.
(49) Tamamizu, S.; Guzman, G. R.; Santiago, J.; Rojas, L. V.; McNamee, M. G.; Lasalde-Dominicci, J. A. Functional Effects of Periodic Tryptophan Substitutions in the Alpha M4 Transmembrane Domain of the Torpedo Californica Nicotinic Acetylcholine Receptor. *Biochemistry* **2000**, *39*, 4666−4673.
(50) Lobo, I. A.; Trudell, J. R.; Harris, R. A. Cross-Linking of Glycine Receptor Transmembrane Segments Two and Three Alters Coupling of Ligand Binding With Channel Opening. *J. Neurochem.* **2004**, *90*, 962−969.
(51) Eger, E. I., II.; Ionescu, P.; Laster, M. J.; Fang, Z.; Gong, D.; Chortkoff, B. S.; Hudlicky, T.; Kendig, J. J.; Harris, R. A.; Trudell, J. R.; Pohorille, A. Minimum Alveolar Anesthetic Concentration of Fluorinated Alkanols in Rats: Relevance to Theories of Narcosis. *Anesth. Analg.* **1999**, *88*, 877−883.
(52) Koblin, D. D.; Chortkoff, B. S.; Laster, M. J.; Eger, E. I., II.; Halsey, M. J.; Ionescu, P. Polyhalogenated and Perfluorinated Compounds That Disobey the Meyer-Overton Hypothesis. *Anesth. Analg.* **1994**, *79*, 1043−1048.
(53) Sonner, J.; Antognini, J. F.; Dutton, R. C.; Flood, P.; Gray, A. T.; Harris, R. A.; Homanics, G. E.; Kendig, J. J.; Orser, B.; Raines, D. E.; Trudell, J. R.; Vissel, B.; Eger, E. I., II Inhaled Anesthetics and Immobility: Mechanisms, Mysteries, and Minimum Aveolar Anesthetic Concentration. *Anesth. Analg.* **2003**, *97*, 718−740.
(54) Pratt, M. B.; Husain, S. S.; Miller, K. W.; Cohen, J. B. Identification of Sites of Incorporation in the Nicotinic Acetylcholine Receptor of a Photoactivatible General Anesthetic. *J. Biol. Chem.* **2000**, *275*, 29441−29451.
(55) Ziebell, M. R.; Nirthanan, S.; Husain, S. S.; Miller, K. W.; Cohen, J. B. Identification of Binding Sites in the Nicotinic Acetylcholine Receptor for [3H]Azietomidate, a Photoactivatable General Anesthetic. *J. Biol. Chem.* **2004**, *279*, 17640−17649.
(56) Chiara, D. C.; Dangott, L. J.; Eckenhoff, R. G.; Cohen, J. B. Identification of Nicotinic Acetylcholine Receptor Amino Acids Photolabeled by the Volatile Anesthetic Halothane. *Biochemistry* **2003**, *42*, 13457−13467.
(57) Barrantes, F. J. Modulation of Nicotinic Acetylcholine Receptor Function Through the Outer and Middle Rings of Transmembrane Domains. *Curr. Opin. Drug Discov. Devel.* **2003**, *6*, 620−632.

CI0497399